Journal of Coastal Research	SI 56	327 - 331	ICS2009 (Proceedings)	Portugal	ISSN 0749-0258

Aeolian Saltation at Esposende Beach, Portugal

B. Li† , H. M. Granja‡, E. J. Farrell†, J. T. Ellis†∞ and D. J. Sherman†

†Department of Geography
Texas A&M University, College Station
TX 77843, USA
libl@geog.tamu.edu
ejfarrell@neo.tamu.edu
sherman@geog.tamu.edu

‡Departamento de Ciências da Terra
Universidade do Minho, 4710-057, Braga
Portugal
hgranja@dct.uminho.pt

∞ Department of Geography,
University of South Carolina, Columbia,
SC 29208, USA
jtellis@mailbox.sc.edu

ABSTRACT

LI, B., GRANJA, H.M., FARRELL, E.J., ELLIS, J.T. and SHERMAN, D.J., 2009. Aeolian saltation at Esposende beach, Journal of Coastal Research, SI 56 (Proceedings of the 10th International Coastal Symposium), 327 – 331. Lisbon, Portugal, ISSN 0749-0258

This paper reports results from a field experiment at Esposende Beach, Portugal, conducted in May/June, 2006. The purpose of the experiment was to measure characteristics of the aeolian saltation system, including sand transport rates, vertical distribution of mass-flux, and the associated wind speeds. The measurements were made on a sand flat, near the top of a parabolic dune flat. The mean grain size of the surface sediments was 0.32 mm. There was an unobstructed fetch exceeding 60 m in length and sloping at approximately 10^o. Sand transport was measured with vertical stacks of hose-type traps and wind profiles were measured with a vertical array of three or four, Gill-type, cup anemometers. The transport rate data are compared to predictions made with the BAGNOLD (1936), KAWAMURA (1951) and ZINGG (1953) models. Vertical flux profiles were analyzed using a geometrically-weighted, trap centering method; using 1 mm as an estimated apparent roughness length, and by fitting a non-linear least-squares curve to find the empirical constants to describe the exponential decay of saltation intensity away from the sand surface. For the 13 data runs that we examined, α averaged 18.663 and β averaged -0.016. These constants yielded an r^2 of 0.992 and an error sum of squares of 1.897 for our data.

ADDITIONAL INDEX WORDS: *Sediment transport, concentration profiles*

INTRODUCTION

One aim of aeolian geomorphology is the development of a process-based understanding of sand transport as a precursor to modeling transport rates and, ultimately, the evolution of aeolian sedimentary environments. Dynamical prediction of morphological responses, from the scales of aeolian bedforms to dunes and dune assemblages, requires the ability to accurately model sediment transport rates based upon wind velocities and sediment surface properties. However, commonly used transport models (BAGNOLD, 1936; KAWAMURA, 1951; ZINGG, 1953) are not in good agreement with observed field measurements (NAMIKAS and SHERMAN, 1998; WIGGS *et al.*, 2004). SHERMAN *et al.* (1998) evaluated the performance of five physically-based models and argued that KAWAMURA model predicts the greatest transport rates, the ZINGG model the least, and the BAGNOLD model is the moderate. The predicted transport rate from KAWAMURA's model can be about 700% to 800% more than the lowest estimation from ZINGG's model. These discrepancies may come from the complex conditions in the field, such as the fetch of the sand surface (NORDSTROM and JACKSON, 1992; JACKSON and COOPER, 1999; BAUER and DAVIDSON-ARNOTT, 2003), sediment moisture content (BELLY, 1964; NAMIKAS and SHERMAN, 1995; CORNELIS and GABRIELS, 2003; WIGGS *et al.*, 2004; BAUER *et al.*, In Press), differences in sediment size populations (BAUER, 1991; RASMUSSEN and SØRENSEN, 1999), presence of vegetation (NIEDORODA *et al.*, 1991; LANCASTER and BAAS, 1998; ARENS *et al.*, 2001; KURIYAMA *et al.*, 2005), and local morphological characteristics (HESP *et al.*, 2005). These discrepancies may reflect the application of inadequately-scaled laboratory relationships to natural environments (SHERMAN and FARRELL, 2008). In conditions where there is a lack of local information, SHERMAN *et al.* (2005) propose a protocol to predict the maximum and minimum transport potentials to assist dune or beach management or risk mitigation.

Because most wind-blown sand is moved via saltation (rather than reptation or suspension), grain trajectory plays a fundamental role in the transport process. Understanding the nature of these trajectories is therefore central to the development of physics-based models for predicting transport rates and related phenomena. For the physically-based transport models (e.g., BAGNOLD, 1936; KAWAMURA, 1951), the vertical characteristic concentration profile (ZINGG, 1953; BUTTERFIELD, 1999; DONG *et al.*, 2006), a bulk representation of saltation trajectories, provides a basis for those transport models. Three main types of functions have been used to describe the profile gradient: power (ZINGG, 1953; BUTTERFIELD, 1999), logarithmic (RASMUSSEN and MIKKELSEN, 1998), and exponential (GREELEY *et al.*, 1996; DONG *et al.*, 2003; NAMIKAS, 2003). The lack of agreement over a basic physical process is surprising. We believe that the inconsistent application of functions results from misrepresenting non-point trap elevations, erroneous regression analysis, or inadequate bed elevation measurements. ELLIS *et al.* (In Review) proposed a standard protocol to measure, analyze, and characterize the vertical mass flux by using geometrically-weighted trap centering, an estimated apparent roughness length, and by fitting a non-linear least-squares curve to find the empirical constants to describe the exponential decay of saltation away from the sand surface.

The purpose of this paper is to report the results of saltation experiments designed to obtain measurements and derivations for wind shear velocities, sediment characteristics, sediment transport rates, and vertical mass flux profiles. The vertical mass flux profiles will be analyzed using the standardized protocol of ELLIS *et al.* (In Review). Our analysis will help assess the applicability of this protocol using a range of transport conditions. Measured sediment transport rates will be compared to common transport models and tested against the ranging method described by SHERMAN *et al.* (2005).

METHODS

Data collection

The study site was on a non-vegetated sand surface near the top of a parabolic dune flat at Esposende Beach, Portugal. The unobstructed fetch exceeded 60 m, sloping at approximately 10^o. The experiments were conducted in May/June 2006. Atmospheric conditions were dry throughout the experiments. The sand transport and mass-flux profile measurements were collected during 13 data runs with arrays of seven, vertically stacked hose-style traps (PEASE *et al.*, 2002). The size of the vertical openings was not constant, with large openings used higher in the arrays. Traps 1 and 2 (the lowest traps) were 25 mm high. Trap 3 was 50 mm high, except during Runs 1b and 2b, when it was 25mm. Trap 4 was 100 mm high, except during Run 1b, when it was 25 mm high, and Runs 1a, and 2a, when it was 50 mm high. Traps 5, 6, and 7 always had openings 100 mm high. All the traps were 100 mm wide. Each run lasted 10 to 30 min, and sand samples from each trap were weighed to obtain the mass flux vertical distribution. Samples over 50 g were dry-sieved at 0.25 phi intervals to obtain the distribution of grain sizes. Mean grain sizes (*d* in Table 1) varied from 0.27 mm to 0.35 mm, with an overall mean of 0.32 mm. All of the samples were moderately-well to well sorted.

Wind velocities were measured with vertical arrays of either 3 or 4 Gill type, 3-cup anemometers. The anemometers were placed at 0.25, 0.50, and 0.75 m during the three instrument deployment, and an additional anemometer was placed at 1.00 m during the four anemometer deployment. The sampling rate was 5 Hz. During some runs, two vertical stacks of hose traps, located 0.50 m on each side of the anemometer array, were deployed for comparative purposes.

Data Analysis Methods

Shear velocity

Wind velocities for each anemometer were averaged over durations synchronous with hose trap sampling periods and the vertical distributions analyzed with linear regression to solve for shear velocity, $u_* = s/\kappa$, where s is the slope of the least squares regression line and κ is the von Karman constant (BAUER *et al.*, 1992). Summary data are presented in Table 1. Data acquisition problems prevented shear velocity (u_*) analysis during four runs (3a, 3b, 4, and 9). The quality of shear velocity estimates are assessed using the r^2 values from the regression analysis. Except for runs 5 (r^2 = 0.987) and 8 (r^2 = 0.977), the regression coefficients are greater than 0.990.

Sediment transport rate

Three models based upon the measured shear velocities and grain size statistics were used to predict sediment transport rates: KAWAMURA (1951), BAGNOLD (1936), and ZINGG (1953). According to SHERMAN *et al.* (2005), these models can be adopted to predict the maximum, moderate, and minimum transport rates, respectively, under dry conditions.

BAGNOLD'S (1936) model is widely used because of its early derivation and simple form:

$$q = c\sqrt{\frac{d}{D}}\frac{\rho}{g}(u_*^{'})^3 \qquad (1)$$

where q is the transport rate (kg/m/s), c is a constant (1.8 for natural graded dune sands), d is a reference grain diameter of 0.25 mm, ρ is air density (1.2 kg/m^3), g is gravitational acceleration (9.81 m/s^2), $u_*^{'}$ is the wind shear velocity (m/s) under the condition that $u_* > u_{*t}$, and u_{*t} is the threshold shear velocity (m/s) for the initiation of particle motion (Eqn. 4).

KAWAMURA (1951) added an explicit threshold shear velocity into his model:

$$q = c\frac{\rho}{g}(u_* - u_{*t})(u_* + u_{*t})^2 \qquad (2)$$

where the typical c value is 2.78.

ZINGG (1953) modified BAGNOLD's equation and proposed:

$$q = c(\frac{d}{D})^{3/4}\frac{\rho}{g}(u_*^{'})^3 \qquad (3)$$

where c = 0.83.

The sediment transport potential predicted by Eqns. 1-3 will be compared to the observed sediment transport rates based on the total mass flux caught by the hose trap stacks divided by run duration time and corrected for trap width.

Threshold shear velocity

Most considerations of threshold shear velocity follow BAGNOLD'S (1936) classic, physics-based formula:

$$u_{*t} = A\sqrt{gd(\frac{\rho_s - \rho}{\rho})} \qquad (4)$$

where A is a constant, with typical value of 0.01 for the fluid-based threshold and 0.085 for the impact threshold to be used with saltation, and ρ is sediment density (2,650 kg/m^3). Sediment moisture or vegetation modifies the apparent threshold shear velocity, but these issues are not critical at this study site.

Slope correction

BAGNOLD (1973) argued that downslope conditions increase transport rates while upslope conditions decrease them. He suggested correcting transport rate predictions by multiplying with a slope parameter G:

$$G = \frac{\tan\alpha}{\cos\theta(\tan\alpha + \tan\theta)} \qquad (5)$$

where α is the angle of internal friction (about 32°), θ is the surface slope angle (here 10°), and positive values indicate upslope conditions. For our case, G is 0.79, so that uncorrected, predicted transport rates would be about 126% too fast.

Normalized vertical flux profile

For comparison purposes, vertical mass fluxes should be reported as relative values rather than absolute masses. There is no standard normalization method. For example, CHEN *et al.* (1996) and DONG AND QIAN (2007) normalized using total flux, whereas BUTTERFIELD (1999) used flux measured nearest to the bed. In our case, because the hose traps have non-uniform sizes, normalization should also include each individual trap size (height), therefore:

$$Q_{ni} = \left[\frac{Q_i}{Q} / (h_{ti} - h_{bi}) \right] 100 \qquad (6)$$

where Q_{ni} is the normalized flux percent per 10 mm of the opening height of trap *i*, Q_i is the mass flux caught by a given trap, Q is the total mass flux measured during the run, and h_{ti} and h_{bi} are the elevations of the top (*t*) and bottom (*b*) of trap *i*.

For sand traps such as those used here, vertical normalized flux profiles require a proper centering method, regression method, and a fitting function to determine the best fit. ELLIS *et al.* (In Review) compared different centering, regression, and fitting approaches, and proposed a protocol to describe the vertical normalized flux profiles: geometric centering, non-linear least square method, and an exponential function. That protocol is adopted here. The geometric center height (h_g) is derived using:

$$h_g = \sqrt{h_t \cdot h_b} \qquad (7)$$

The upper and lower thickness of the hose traps (5 mm) cannot be neglected when calculating h_g. Therefore, h_t = 25 mm for Trap 1 and h_b = 35 mm for Trap 2, for example. For our trap deployment, h_b = 0 for Trap 1, with a geometric mean of 0 mm. To overcome this mathematical challenge, the apparent roughness length (typical value = 1 mm) was used to calculate h_g (results shown in Table 1). The fitting function to describe the mass-flux gradient follows the exponential decay:

$$Q_n = \alpha e^{\beta h} \qquad (8)$$

where α and β are the regression coefficients, Q_n is the normalized flux (in % per 10 mm), and h is the elevation (in mm) of any point above the surface.

Table 1: Mean grain size (*d*), shear velocity (u_*), threshold shear velocity (u_{*t}), sediment flux (Q), and normalized flux (Q_{ni}) for each run.

Run	*d* (mm)	u_* (m/s)	u_{*t} (m/s)		Trap 1	Trap 2	Trap 3	Trap 4	Trap 5	Trap 6	Trap 7
Run 1a	0.31	0.49	0.22	Q (g)	268.87	99.63	92.28	40.69	15.31	5.65	0.60
				Q_{ni} (% per 10 mm)	20.56	7.62	3.53	1.56	0.29	0.11	0 .01
Run 1b	0.31	0.49	0.22	Q (g)	243.14	79.95	44.18	25.25	22.84	20.37	3.37
				Q_{ni} (% per 10 mm)	22.15	7.28	4.02	2.30	0.52	0.46	0.08
Run 2a	0.31	0.41	0.22	Q (g)	63.77	31.42	32.09	10.61	5.84	1.25	0.32
				Q_{ni} (% per 10 mm)	17.56	8.65	4.42	1.46	0.40	0.09	0.02
Run 2b	0.30	0.41	0.21	Q (g)	64.87	46.57	23.7	15.12	1.09	0.59	0.00
				Q_{ni} (% per 10 mm)	17.08	12.26	6.24	1.00	0.07	0.04	0.00
Run 3a	0.32	N/A	0.22	Q (g)	160.11	53.54	45.73	25.52	20.65	4.69	0.63
				Q_{ni} (% per 10 mm)	20.6	6.89	2.94	1.64	0.66	0.15	0.02
Run 3b	0.32	N/A	0.22	Q (g)	167.1	77.56	45.87	42.7	1.45	1.51	0.14
				Q_{ni} (% per 10 mm)	19.87	9.22	5.46	1.27	0.04	0.04	0.00
Run 4	0.35	N/A	0.24	Q (g)	333.35	153.75	182.91	106.52	31.73	8.25	0.00
				Q_{ni} (% per 10 mm)	16.33	7.53	4.48	1.3	0.39	0.1	0.00
Run 5	0.35	0.41	0.24	Q (g)	444.53	335.88	281.85	176.06	48.31	8.05	1.32
				Q_{ni} (% per 10 mm)	13.72	10.37	4.35	1.36	0.37	0.06	0.01
Run 6	0.34	0.35	0.23	Q (g)	150.27	78.04	75.30	54.00	12.19	2.03	0.59
				Q_{ni} (% per 10 mm)	16.14	8.38	4.04	1.45	0.33	0.05	0.02
Run 7	0.33	0.38	0.23	Q (g)	76.93	47.45	38.87	28.28	6.22	1.42	0.00
				Q_{ni} (% per 10 mm)	15.45	9.53	3.90	1.42	0.31	0.07	0.00
Run 8	0.33	0.39	0.23	Q (g)	57.30	34.22	32.71	22.41	5.63	1.06	0.26
				Q_{ni} (% per 10 mm)	14.92	8.91	4.26	1.46	0.37	0.07	0.02
Run 9	0.31	N/A	0.22	Q (g)	68.49	56.68	53.32	39.59	6.05	1.55	0.22
				Q_{ni} (% per 10 mm)	12.13	10.04	4.72	1.75	0.27	0.07	0.01
Run 10	0.27	0.38	0.21	Q (g)	51.60	33.05	37.88	15.59	3.52	0.66	0.21
				Q_{ni} (% per 10 mm)	14.48	9.28	5.32	1.09	0.25	0.05	0.01

RESULTS AND ANALYSIS

Shear velocities and threshold shear velocities are summarized in Table 1. Some runs have two vertical arrays of hose traps (labeled *a* and *b*) that share the same wind data. Shear velocities ranged between 0.35 and 0.49 m/s. Threshold shear velocities varied only slightly (between 0.23 and 0.26 m/s) because of the small range of mean particle size.

The slope-corrected (Eqn. 5) sediment transport rates from the BAGNOLD (1936; Eqn. 1), KAWAMURA (1951; Eqn. 2) and ZINGG (1953; Eqn. 3) models, together with the observed data in this field experiment, are plotted in Figure 1.

The three models show similar patterns of transport rates for the study conditions. However, KAWAMURA's model predicts about 220% to 320% faster sediment transport rates than those associated with ZINGG's model. Our measured transport rates were generally less than those predicted by any of the models except during Runs 3 and 4. The average sediment transport rates predicted by the BAGNOLD, KAWAMURA, and ZINGG models and those observed are 0.011, 0.020, 0.007, and 0.005 kg/m/s, respectively. ZINGG's predictions are similar in magnitude to the observed data and the mean values are only slightly different. Our results indicate that the protocol SHERMAN *et al.* (2005) proposed is not applicable in this environment.

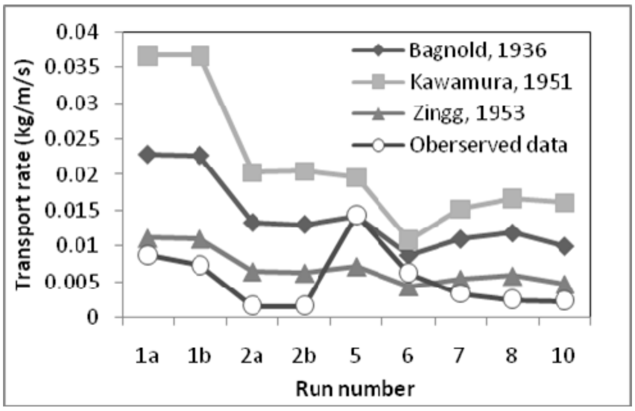

Figure 1. Predicted and observed sediment transport rates

The results of the curve fitting using the ELLIS *et al.* (In Review) protocol are shown in Table 2. Implementing the nonlinear least squared, exponential curve fitting using the geometric centering method yields high regression coefficients [$\overline{r^2}$ = 0.992, $\sigma(\overline{r^2})$ = 0.009] and a low error sum of squares [$\overline{SSE}$ = 1.897, $\sigma(\overline{SSE})$ = 2.002]. The fitting coefficients (α and β) have ranges of 13.517 to 24.782 and -0.010 to -0.024, respectively, and the standard deviations are 17.8% and 27.0% of the absolute mean values. We are uncertain about the cause of this variability, but it is likely due to a combination of changes in shear velocity, grain size, and the occurrence of non-equilibrium saltation events.

DISCUSSION AND CONCLUSIONS

Figure 2 shows the normalized flux profiles from this study and from experiments conducted in at Guadalupe, CA, USA. For the Guadalupe data (described in ELLIS *et al.*, In Review) the mean grain size was 0.39 mm. For each site we have plotted the mean exponential distribution based upon averaging values of α and β from individual runs. The largest difference between normalized flux profiles for the Esposende and Guadalupe distributions is 5% per 10 mm at the surface. The differences are minor at elevations above 20 mm and below about 70 mm (less than 1% difference per 10 mm). Above 70 mm the differences increase again up to about 180 mm and then drops to less than 1% over the rest of the distribution. The overall similarity of flux distributions between these two aeolian environments reinforces a belief that there is an ideal flux profile.

Table 2: Characteristics of exponential distributions.

Run #	r^2	*SSE*	α	β
1a	0.996	1.376	22.771	-0.022
1b	0.994	2.120	24.782	-0.024
2a	0.999	0.131	19.006	-0.017
2b	0.974	7.437	19.090	-0.013
3a	0.993	2.241	23.106	-0.024
3b	0.999	0.393	21.702	-0.018
4	0.995	1.043	17.478	-0.016
5	0.980	3.721	15.190	-0.012
6	0.999	0.125	17.402	-0.016
7	0.995	1.073	16.828	-0.014
8	0.999	0.223	16.098	-0.014
9	0.975	3.874	13.517	-0.010
10	0.995	0.899	15.653	-0.012
Mean	0.992	1.897	18.663	-0.016
St. Dev.	0.009	2.002	3.330	0.004

The sediment transport potential range that SHERMAN *et al.* (2005) proposed has been evaluated using 9 runs in which saltation and wind were measured on the top of a parabolic coastal dune at Esposende, Portugal. The results indicate that the protocol overestimates the range of the sediment transport for most of runs except runs 5 and 6. However, for long-term applications, the protocol provides a relative acceptable range of sediment transport rates if we have approximations for wind, sediment, weather, and topography conditions. After applying the protocol of ELLIS *et al.* (In Review) to the Esposende and Guadalupe data we found that the normalized vertical flux profiles are quite similar. This supports our contention that the ELLIS *et al.* (In Review) protocol is a feasible method to standardize findings so that we can compare vertical saltation mass flux under different environmental conditions. The range of the normalized profiles that we found for the Esposende data suggest that either our field protocol was not controlled tightly enough or that there are environmental controls that we are not accounting for. In particular, some of the variability may be associated with fluctuations in the saltation system

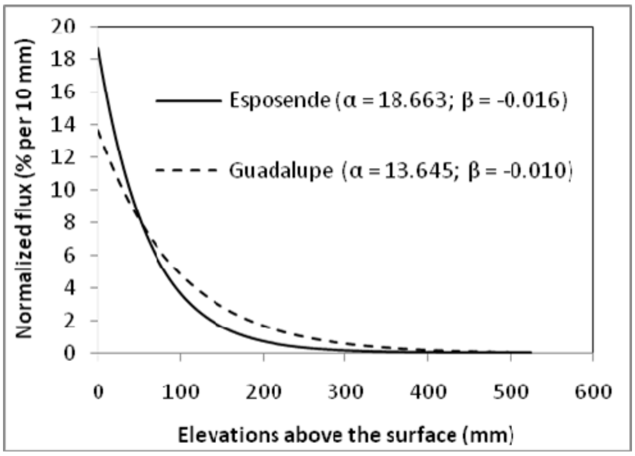

Figure 2. Comparison of the normalized flux profiles from two environments.

occuring at time scales shorter than our averaging intervals (e.g., ELLIS, 2006).

In any field experiment there are always uncertain, unobservable, or uncontrollable factors that introduce variability to results. For example, decades of field research have failed to yield observations that match predictions for our transport models. We still seek resolution of these factors. We have found success with measuring and describing saltation profiles, but less success with matching observed and predicted sand transport rates.

LITERATURE CITED

ARENS, S.M.; BAAS, A.C.W.; VAN BOXEL, J.H., and KALKMAN, C., 2001, Influence of reed stem density on foredune development. *Earth Surface Processes and Landforms*, 26(11), 1161-1176.

BAGNOLD, R.A., 1936, The movement of desert sand. *Proceedings of the Royal Society of London, Series A*, 157, 594-620.

BAGNOLD, R.A., 1973, The nature of saltation and 'bed-load' transport in water. *Proceedings of the Royal Society of London*, 332, 473-504.

BAUER, B.O., 1991, Aeolian decoupling of beach sediments. *Annals of Association of American Geographers*, 81(2), 290-303.

BAUER, B.O. and DAVIDSON-ARNOTT, R.G.D., 2003, A general framework for modeling sediment supply to coastal dunes including wind angle, beach geometry, and fetch effects. *Geomorphology*, 49(1), 89-108.

BAUER, B.O.; DAVIDSON-ARNOTT, R.G.D.; HESP, P.A.; NAMIKAS, S.L.; OLLERHEAD, J., and WALKER, I.J., In Press, Aeolian sediment transport on a beach: Surface moisture, wind fetch, and mean transport. *Geomorphology*.

BELLY, P.Y., 1964, Sand movement by wind, *Coastal Engineering Research Center Technical Memorandum*: U.S. Army Corps of Engineers, Vol. 1, 38 p.

BUTTERFIELD, G.R., 1999, Application of thermal anemometry and high-frequency measurement of mass flux to aeolian sediment transport research. *Geomorphology*, 29(1-2), 31-58.

CHEN, W.; YANG, Z.; ZHANG, J., and HAN, Z., 1996, Vertical distribution of wind-blown sand flux in the surface layer, Taklamakan Desert, Central Asia. *Physical Geography*, 17(3), 193-218.

CORNELIS, W.M. and GABRIELS, D., 2003, The effect of surface moisture on the entrainment of dune sand by wind: An evaluation of selected models. *Sedimentology*, 50(4), 771-790.

DONG, Z.; LIU, X.; WANG, H., and WANG, X., 2003, Aeolian sand transport: A wind tunnel model. *Sedimentary Geology*, 161(1-2), 71-83.

DONG, Z. and QIAN, G., 2007, Characterizing the height profile of the flux of wind-eroded sediment. *Environmental Geology*, 51(5), 835-845.

DONG, Z.; QIAN, G.; LUO, W., and WANG, H., 2006, Analysis of the mass flux profiles of an aeolian saltating cloud. *Journal of Geophysical Re*search, 111, D16111.

ELLIS, J.T., 2006, Coherent Structures and Aeolian Saltation. Ph.D. Dissertation, Texas A&M University, 123 p.

ELLIS, J.T.; LI, B.; FARRELL, E.J., and SHERMAN, D.J., In Review, Protocols for characterizing aeolian mass-flux profiles. *Aeolian Research*.

GREELEY, R.; BLUMBERG, D.G., and WILLIAMS, S.H., 1996, Field measurements of the flux and speed of wind-blown sand. *Sedimentology*, 43(1), 41-52.

HESP, P.A.; DAVIDSON-ARNOTT, R.; WALKER, I.J., and OLLERHEAD, J., 2005, Flow dynamics over a foredune at Prince Edward Island, Canada. *Geomorphology*, 65(1-2), 71-84.

JACKSON, D.W.T. and COOPER, J.A.G., 1999, Formation of ephemeral bedform turrets in coastal foredunes. *Journal of Geology*, 107(5), 633-639.

KAWAMURA, R., 1951, Study of sand movement by wind. Institute of Science and Technology, University of Tokyo, Technical Reports, Vol. 5, No. 34. Translated as *University of California Hydraulics Engineering Laboratory Report HEL 2-8*, 1964.

KURIYAMA, Y.; MOCHIZUKI, N., and NAKASHIMA, T., 2005, Influence of vegetation on aeolian sand transport rate from a backshore to a foredune at Hasaki, Japan. *Sedimentology*, 52(5), 1123-1132.

LANCASTER, N. and BAAS, A., 1998, Influence of vegetation cover on sand transport by wind: Field studies at Owens Lake, California. *Earth Surface Processes and Landforms*, 23(1), 69-82.

NAMIKAS, S. and SHERMAN, D., 1995, A review of the effects of surface moisture content on aeolian sand transport. In: Tchakerian, V., (ed.), *Desert Aeolian Processes*: London: Chapman and Hall, pp. 269-293.

NAMIKAS, S. and SHERMAN, D., 1998, AEOLUS II: an interactive program for the simulation of aeolian sedimentation. *Geomorphology*, 22(2), 135-149.

NAMIKAS, S.L., 2003, Field measurement and numerical modeling of aeolian mass flux distributions on a sandy beach. *Sedimentology*, 50(2), 303-326.

NIEDORODA, A.W.; SHEPPARD, D.M., and DEVEREAUX, A.B., 1991, Effect of beach vegetation on aeolian sand transport. *Coastal Sediments '91*, pp. 246-260.

NORDSTROM, K.F. and JACKSON, N.L., 1992, Effect of source width and tidal elevation changes on aeolian transport on an estuarine beach. *Sedimentology*, 39(5), 769-778.

PEASE, P.; GARES, P., and LECCE, S., 2002, Eolian dust erosion from an agricultural field on the North Carolina Coastal Plain. *Physical Geography*, 23(5), 381-400.

RASMUSSEN, K.R. and SØRENSEN, M., 1999, Aeolian mass transport near the saltation threshold. *Earth Surface Processes and Landforms*, 24(5), 413-422.

SHERMAN, D.; Jackson, D.; Namikas, S., and Wang, J., 1998, Wind-blown sand on beaches: an evaluation of models. *Geomorphology*, 22(2), 113-133.

SHERMAN, D. and FARRELL, E., 2008, Aerodynamic roughness lengths over movable beds: Comparison of wind tunnel and field data. *Journal of Geophysical Research*, 113, F02S08.

SHERMAN, D.J.; JACKSON, N.L.; NORDSTROM, K.F.; HESP, P.A., and ARENS, S.M., 2005, Predicting maximum and minimum aeolian sand transport rates to provide a basis for assessing management actions for beaches and dunes. In: Sanjaume, E., and Mateu, J., (eds.), *Geomorfologia litoral I Quaternari: Homenatge al Professor V.M. Rosselló*: Valencia University Press, Spain, pp. 483-496.

WIGGS, G.F.S.; BAIRD, A.J., and ATHERTON, R.J., 2004, The dynamic effects of moisture on the entrainment and transport of sand by wind. *Geomorphology*, 59(1-4), 13-30.

ZINGG, A.W., 1953, Wind tunnel study of the movement of sedimentary material. *Proceedings of the 5th Hydraulics Conference* (Iowa City), Vol. 34, pp. 111-135